Materials Horizons

Rational Mechanochemical Design of Diels–Alder Crosslinked Biocompatible Hydrogels with Enhanced Properties

Journal:	*Materials Horizons*
Manuscript ID	MH-COM-03-2022-000338.R1
Article Type:	Communication
Date Submitted by the Author:	24-Apr-2022

Complete List of Authors:	Bailey, Sophia; University of California Santa Barbara, Chemistry and Biochemistry Barney, Christopher; University of California Santa Barbara, Mechanical Engineering; University of California Santa Barbara, Chemical Engineering Sinha, Nairiti; University of California Santa Barbara, Chemical Engineering; University of California Santa Barbara, Materials Research Laboratory Pingali, Sai Venkatesh; Oak Ridge National Laboratory, Biology and Soft Matter Division Hawker, Craig; University of California Santa Barbara, Chemistry and Biochemistry; University of California Santa Barbara, Materials Research Laboratory; University of California Santa Barbara, Materials Helgeson, Matthew; University of California Santa Barbara, Chemical Engineering Valentine, Megan; University of California Santa Barbara, Mechanical Engineering Read de Alaniz, Javier; University of California Santa Barbara, Chemistry and Biochemistry

New Concepts

In this manuscript, we establish molecular mechanochemical design principles for Diels–Alder (DA) crosslinked polymer networks to improve macroscopic failure properties. To-date, DA-based hydrogels typically rely on the cycloaddition between furan and maleimide, where molecular-level design has either focused on the thermal cycloreversion to afford delivery systems or cycloaddition kinetics to enable rapid gelation for cell encapsulation. The consideration of the mechanically induced cycloreversion, however, has yet to be explored as a strategy to improve material properties or applications. Herein, we employ constrained geometries simulate external force computational methods, to identify "mechanoresistant" DA adducts with reduced mechanochemical activity over the traditional "mechanolabile" furan–maleimide system. Impressively, when these "mechanoresistant" crosslinks are employed within tetraPEG hydrogels, a nearly 3-fold increase in puncture resistance is observed over the traditional furan–maleimide system. Furthermore, through combined mechanochemical and kinetic design principles we present a new diene for rapid gelation applications (< 5 min) that also imparts improved material toughness. Given the ubiquity of DA cycloadditions in the preparation of hydrogels for a variety of biological applications, this new molecular design principle will enable access to mechanically robust hydrogels and could provide great potential in the design of dynamic biomimetic materials.

Rational Mechanochemical Design of Diels–Alder Crosslinked Biocompatible Hydrogels with Enhanced Properties

Sophia J. Bailey,[a] Christopher W. Barney,[b,c] Nairiti J. Sinha,[c,d] Sai Venkatesh Pangali,[e] Craig J. Hawker,[a,c,f] Matthew E. Helgeson,[c] Megan T. Valentine[b] and Javier Read de Alaniz*[a]

[a.]Department of Chemistry and Biochemistry, University of California Santa Barbara, Santa Barbara, CA 93106.
[b.]Department of Mechanical Engineering, University of California Santa Barbara, Santa Barbara, CA 93106.
[c.]Department of Chemical Engineering, University of California Santa Barbara, Santa Barbara, CA 93106.
[d.]Materials Research Laboratory, University of California Santa Barbara, Santa Barbara, CA 93106.
[e.]Center for Structural Molecular Biology, Neutron Scattering Division, Oak Ridge National Laboratory, Oak Ridge, TN, 37831.
[f.]Materials Department, University of California Santa Barbara, Santa Barbara, CA 93106.

ABSTRACT

An important but often overlooked feature of Diels–Alder (DA) cycloadditions is the ability for DA adducts to undergo mechanically induced cycloreversion when placed under force. Herein, we demonstrate that the commonly employed DA cycloaddition between furan and maleimide to crosslink hydrogels results in slow gelation kinetics and "mechanolabile" crosslinks that relate to reduced material strength. Through rational computational design, "mechanoresistant" DA adducts were identified by constrained geometries simulate external force models and employed to enhance failure strength of crosslinked hydrogels. Additionally, utilization of a cyclopentadiene derivative, spiro[2.4]hepta-4,6-diene, provided mechanoresistant DA adducts and rapid gelation in minutes at room temperature. This study illustrates that strategic molecular-level design of DA crosslinks can provide biocompatible materials with improved processing, mechanical durability, lifetime, and utility.

Diels–Alder (DA) cycloadditions have found extensive use in drug delivery, biomedical device fabrication and tissue engineering due to their cytocompatible, additive free and efficient click nature.[1,2] In addition to the advantages that DA cycloadditions offer in the construction of materials, the thermal

reversibility has also provided numerous advances in the design of remendable materials,[3] on-demand reactivity,[4,5] and drug delivery systems.[6] While thermal retro-DA (rDA) reactions are well-known and exploited, the *mechanically* induced cycloreversion has only recently been explored.[7–11] Interestingly, mechanochemical reactivity is particularly sensitive to the geometry of a molecule relative to the forces applied; thus, regio- and stereo-isomers of DA adducts have been shown to exhibit notable differences in their ability to undergo mechanically induced cycloreversion.[10,11] Furthermore, the effect of mechanically labile (or mechanolabile) bonds on macroscopic material properties was recently highlighted by Craig and coworkers, who showed that the macroscopic fracture properties of poly(ethylene glycol) (PEG) gels can be directly related to the presence and reactivity of cyclobutane mechanophores as "weak links."[12] However, the direct use of mechanochemical reactivity to improve material properties has yet to be addressed.

In designing biocompatible materials, one inherent drawback of synthetic hydrogels is that they often do not possess the same strength of the natural soft tissues they are designed to interface with or replace. Given that extensive work has been conducted improve the mechanical properties of biocompatible hydrogels,[13–15] we envision that the rational design of DA cycloadducts could provide a facile route to improved strength of materials by structurally modifying the diene–dienophile pairs invoked to prevent mechanically induced rDA reactions (Figure 1a–b). This hypothesis is predicated on the striking difference in threshold forces reported for the mechanically induced rDA between furan regioisomers[10] and the recently reported effect of mechanical bond strength on macroscopic fracture properties.[12,16] In reviewing the multitude of elegant and exciting DA-based biomaterials reported in literature[1,2,17–19] we recognized a striking commonality: furan–maleimide crosslinked biomaterials have exclusively used *proximal* furans. However, this regioisomer is known to provide facile and selective polymer mechanoscission by rDA with maximum force values (F_{max}) of 3.6 and 3.8 nN for *endo* and *exo* isomers, respectively, determined by constrained geometries simulate external force (CoGEF) computational methods.[10] In contrast, the *distal* furan–maleimide regioisomer was reported to possess increased

mechanical resistance (or mechanoresistance), with the F_{max} of the *endo* isomer increasing to 4.3 nN to induce rDA and the *exo* isomer becoming mechanically inert; thus, applied forces resulted in non-selective bond rupture instead of rDA with F_{max} = 5.8 nN.[10] Given the significant difference in mechanolability of these DA adducts, we hypothesized that the failure strength of biocompatible materials could be increased through strategic employment of mechanoresistant DA linkages.

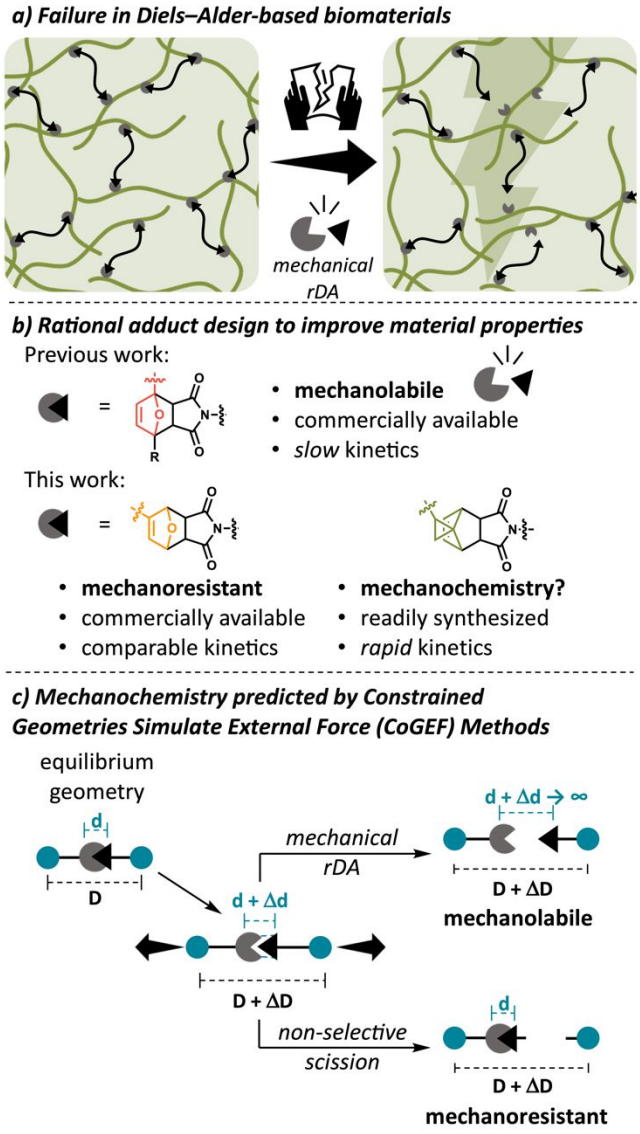

Figure 1. a) Graphical depiction of force-induced material fracture. b) Structures of DA cycloadducts investigated. c) Schematic representation of the CoGEF method.

To elucidate the impact of DA adduct mechanolability on the strength of materials, three dienes were chosen for investigation: *proximal* furan (pFA), mechanoresistant *distal* furan (dFA), and a new cyclopentadiene derivative, spiro[2.4]hepta-4,6-diene (SpCp) with unknown mechanochemical reactivity (Figure 1b). We were particularly interested in the employment of SpCp–maleimide crosslinking as the cycloaddition has a reported second-order rate constant of 2.6 $M^{-1}s^{-1}$ in water,[20] providing promise in rapid gelation applications such as 3D printing[21] and cell encapsulation[19, 22] which are traditionally incompatible with the slow cycloaddition between furan and maleimide. In comparison to cyclopentadiene, attachment of a bulky cyclopropane ring prevents unwanted dimerization of SpCp[23] which provides improved control and long-term storage of functionalized building blocks. Though cyclopentadiene–maleimide adducts require high temperatures (>200 °C) to induce thermal cycloreversion,[24] *proximal* cyclopentadiene–maleimide adducts are reported to undergo mechanical rDA reactions.[25,26] However, we hypothesized that the non-traditional connectivity of the SpCp–maleimide adduct might reduce the ability to transduce forces to the DA bond. Additionally, *gem*-dihalocyclopropane (gDHC) units are known to act as nonscissile mechanophores such that mechanical ring opening dissipates stress in gDHC containing polymers without scission of the main chain.[27] Thus, we envisioned that the cyclopropane unit might also affect the overall mechanolability of SpCp–maleimide.

Table 1. Summary of mechanochemical reactivity of DA adducts determined by CoGEF

	U_{max} (kJ/mol)	F_{max} (nN)	Mechanolabile?
***endo* pFA**	231	3.9	**Yes**
***exo* pFA**	295	4.0	**Yes**
***endo* dFA**	493	4.8	**Yes**
***exo* dFA**	553	5.7	**No**
***endo* SpCp**	492	5.7	**No**
***exo* SpCp**	517	5.7	**No**

To assess the mechanochemical reactivity of SpCp–maleimide we completed a comparative CoGEF investigation on truncated structures of the three adducts we intend to employ within hydrogels following

reported methods (Figure 1c).[28] Plotting the relative energy of each optimized constrained geometry against the displacement (ΔD) from equilibrium afforded the maximum energy before scission (U_{max}) and the slope of CoGEF curves preceding U_{max} provided a measure of the maximum force imparted on the system (F_{max}) (see Supplementary Information Section 5).[28] The calculated U_{max} and F_{max} values for pFA and dFA adducts were in good agreement with previous CoGEF analyses (Table 1, Supplementary Figures S18–20).[10,11,28] As previously reported and depicted in Figure 2a, the stepwise elongation of pFA and dFA–maleimide adducts reveals an exponential increase in the change in bond length (Δd) between furan and maleimide (bond indicated in blue, Figure 2b) for both *endo* and *exo* pFA–maleimide and *endo* dFA–maleimide, indicating preferential cycloreversion to furan and maleimide. In contrast, elongation of *exo* dFA–maleimide results in a plateau and eventual relaxation to initial DA bond length, indicative of non-selective bond rupture (Figure 2a). Notably, elongation of both *endo* and *exo* SpCp–maleimide adducts resulted in the same behavior, again indicating non-selective bond rupture. The implications of these plots are corroborated by each optimized geometry after the simulated scission event by CoGEF. For "mechanolabile" adducts – *endo* pFA, *exo* pFA and *endo* dFA – the scission event results in reformation of furan and maleimide, whereas "mechanoresistant" adducts, *exo* dFA, *endo* SpCp and *exo* SpCp, prompt terminal bond rupture of the truncated structure, indicative of non-selective polymer scission (Figure 2b, Supplementary Figures S18–S20). These results suggest that employment of SpCp–maleimide adducts would provide mechanically robust crosslinks, similar to *distal* furan–maleimide adducts, and in contrast to the pFA–maleimide counterparts.

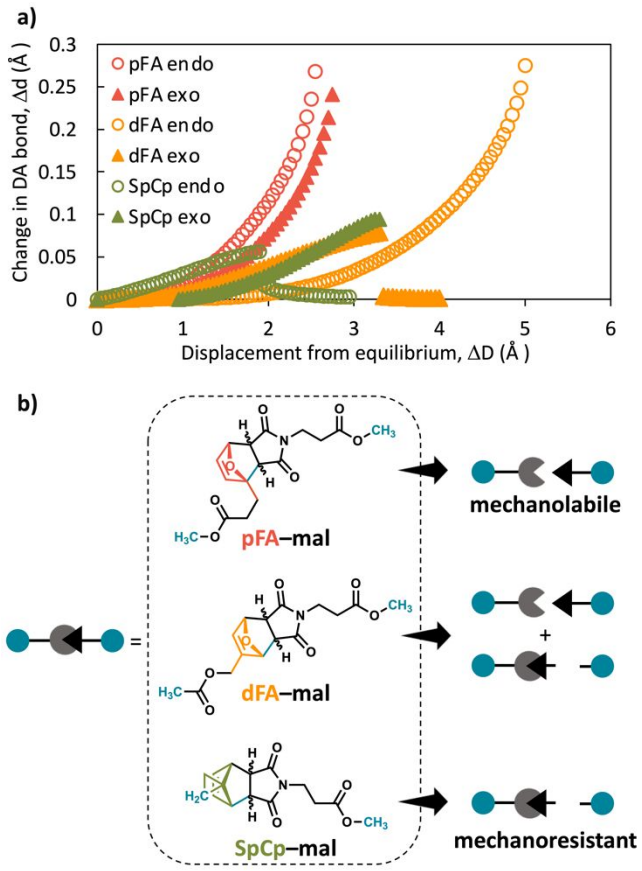

Figure 2. a) Change in DA bond length (Δd) plotted against displacement from equilibrium (ΔD) for each adduct. b) Truncated structures used for CoGEF and graphical depiction of scission route for each adduct.

To validate the computational studies and probe the effect of DA mechanochemical reactivity on failure strength in biologically relevant materials, we prepared PEG hydrogels from DA-based crosslinking of maleimide with pFA, dFA or SpCp. Hydrogels were prepared from crosslinking four armed telechelic maleimide poly(ethylene glycol) (tetramalPEG) (20 kDa) to provide precise control over network structure[29–31] and enable a straightforward comparison of adduct molecular structure on resulting material mechanics. Diene containing crosslinkers were prepared by functionalizing 2 kDa PEG with carboxylic acid containing pFA, dFA and SpCp derivatives (see Supplementary Information Sections 1.2–1.3). TetraPEG hydrogels were then prepared by combining these diene crosslinkers and tetramalPEG at 8 wt%

polymer in water with diene and maleimide groups in stoichiometric balance and allowing to cure at room temperature over 10 days (Figure 3a, Supplementary Information Section 1.4).

Small angle neutron scattering (SANS) measurements on fully cured 8 wt% gels in deuterium oxide (D, 99.9%) were conducted to compare the resulting nanostructures from each diene type. As presented in Figure 3b, SANS curves of the hydrogels indicate signatures consistent with previously reported scattering from tetra-PEG networks,[32,33] but with indistinguishably different structural features for networks prepared with SpCp, pFA or dFA. Notably, the mesh size l was determined to be approximately 60 nm, where $l=2\pi/q^*$ and $q^*\sim 0.01\ Å^{-1}$ is the critical scattering vector below which scattering intensity shows a featureless upturn. The 12 kDa PEG chains have a contour length of approximately 90 nm, so the measured mesh size is consistent with expectations for hydrogels constructed of 12 kDa PEG chains between crosslinks. This similarity of the underlying nanostructure is further corroborated by similarities in the swelling behavior of each hydrogel (Figure 3c, Supplementary Table S2). Some variance in the measured Young's modulus (E) of fully cured hydrogels was observed and attributed to the more efficient crosslinking obtained through SpCp–maleimide which occurs rapidly within minutes, resulting in a final modulus value of 14.5 kPa; by contrast, pFA and dFA networks required 7–10 days to reach comparable modulus values of 10.3 and 11.9 kPa, respectively (Figure 3d). Taken together, these results support that SpCp, pFA and dFA can be used interchangeably without greatly affecting the final morphology of the network, although variance in final modulus values should be considered in the assessment of material failure strength.

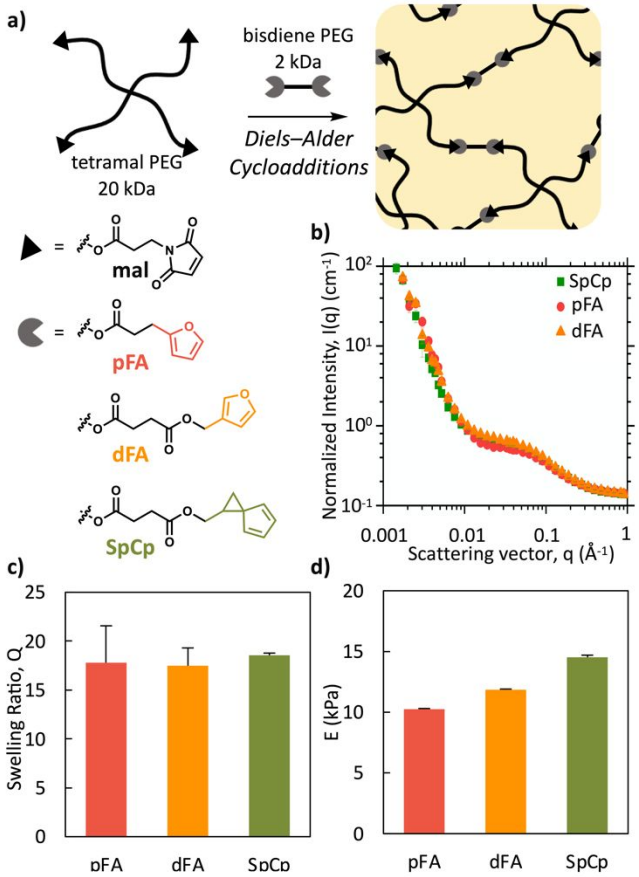

Figure 3. a) Schematic representation of tetraPEG hydrogel formation from crosslinking maleimide-functionalized tetraPEG (20 kDa) with diene functionalized PEG linkers (2 kDa). b) Overlay of SANS plots of fully cured hydrogels prepared at 8 wt% in deuterium oxide. The critical scattering vector q^* is approximately 0.01 Å^{-1} for the three hydrogels, wherein scattering from individual PEG chains between crosslinks dominate for $q>q^*$. c) Equilibrium swelling ratio, Q, for each hydrogel (n = 3). d) Modulus determined by indentation for each hydrogel (n = 6 pFA, n = 4 dFA/SpCp).

The contrasting curing times for furan (pFA/dFA) and cyclopentadiene (SpCp) derived hydrogels were in agreement with reported kinetics of hydrophobic accelerated DA cycloadditions.[20,34] As anticipated, the SpCp containing linker provided rapid gelation, passing a flip-test within 2 minutes (Figure 4a). However, pFA and dFA based hydrogels, which undergo a much slower cycloaddition required 20 h and 42 h to gel, respectively, and multiple days to reach full cure at room temperature as determined by *in situ*

indentation measurements (Figure 4a, Supplementary Table S3). To further compare the efficiency of these cycloadditions, a kinetics study was completed by monitoring the reaction of each diene crosslinker (prepared at 2.5 mM in D_2O) with two equivalents of 3-maleimidopropionic acid by ^1H NMR spectroscopy (Supplementary Information Section 4). Strikingly, the SpCp–maleimide system reached 85% conversion within 5 minutes, and quantitative conversion was confirmed after 30 minutes (Figure 4b). In contrast, the two furan-based crosslinkers exhibit considerably slowed kinetics in agreement with gelation times (Figure 4a) and previous reports.[19,20] Given that SpCp network morphology is comparable to classically employed pFA, the enhanced kinetics and crosslinking efficiency offers a significant advantage for material throughput and for applications such as 3D printing where rapid gelation is desired. Additionally, this study provided insights into the anticipated *endo:exo* ratio of cycloadducts within each hydrogel (Figure 4b, Supplementary Figure S15–S17). This ratio is most important in the case of dFA where the *endo* and *exo* isomers have strikingly different mechanochemical behavior. After 120 h, the *endo*:*exo* ratio for dFA–mal was determined to be 1:0.8, indicating that under room temperature curing conditions nearly half of the formed linkages in our hydrogel will be mechanoresistant *exo* dFA–mal.

Initial investigations into the fracture properties of the tetra-PEG hydrogels were attempted via notch tests; however, multi-day curing was incompatible with preparing the thin film (1 mm) geometries required for this method due to solvent evaporation from molds. Additionally, the low working time of the SpCp samples (less than 2 minutes) prohibited the creation of films with uniform thickness. As an alternative, we identified puncture as a preferable technique that involved facile sample preparation within sealed glass vials, did not require the manipulation of fragile gels, and provided high throughput and repeatable measurements.[35–37] Puncture of samples was accomplished by inserting a blunt needle (359 μm outer radius) into samples with constant displacement rate (1 mm/s) until puncture was achieved (see Supplementary Information Section 2). Here puncture force is used as a relative indicator of the strength of the different samples, as has been done previously.[36] Note that while the puncture force is representative of a material strength, a positive relationship between this quantity and fracture toughness has been

previously observed in experiment[38] and modeling.[39] Further, recent work has suggested a link between bond strength and puncture force.[16] As presented in Figure 4c, significantly different puncture forces were required for dFA and SpCp-based hydrogels compared to pFA, although scattering measurements, Young's moduli and swelling behaviors indicate similar nanostructures. Hydrogels containing mechanolabile pFA–maleimide crosslinks punctured most readily with a required puncture force (F_c) nearly 3 times lower than that required of the dFA and SpCp analogs (Figure 4c). This observation is in agreement with the trends in mechanochemical reactivity predicted from CoGEF calculations. Some difference in F_c can be attributed to the variance of Young's modulus values presented in Figure 3d in addition to the displacement distance of the needle before puncture (d_c). If the weakest bond strengths in the materials were equal, a molecular argument (Supplementary Information Section 2) predicts that having a reduced crosslinking density in the pFA samples relative to the SpCp samples should result in a 22% increase in F_c in the pFA samples, in contrast to the to the observed 72% decrease in F_c. This indicates that the changes in crosslinking density are not sufficiently large to overcome the changes induced by weakening the bonds in the material. Further, from the continuum perspective, deconvoluting the effect of d_c and E on F_c (Supplementary Figure S12, Supplementary Table S4) indicates that the observed increases in puncture force can be primarily attributed to changes in d_c. This finding suggests that F_c can be used in this case as a relative indicator of the mechanoresistance of DA adducts. The increase in F_c observed in the dFA and SpCp relative to the pFA samples indicates an increase in the molecular strength, or conversely a decrease in the mechanochemical reactivity.

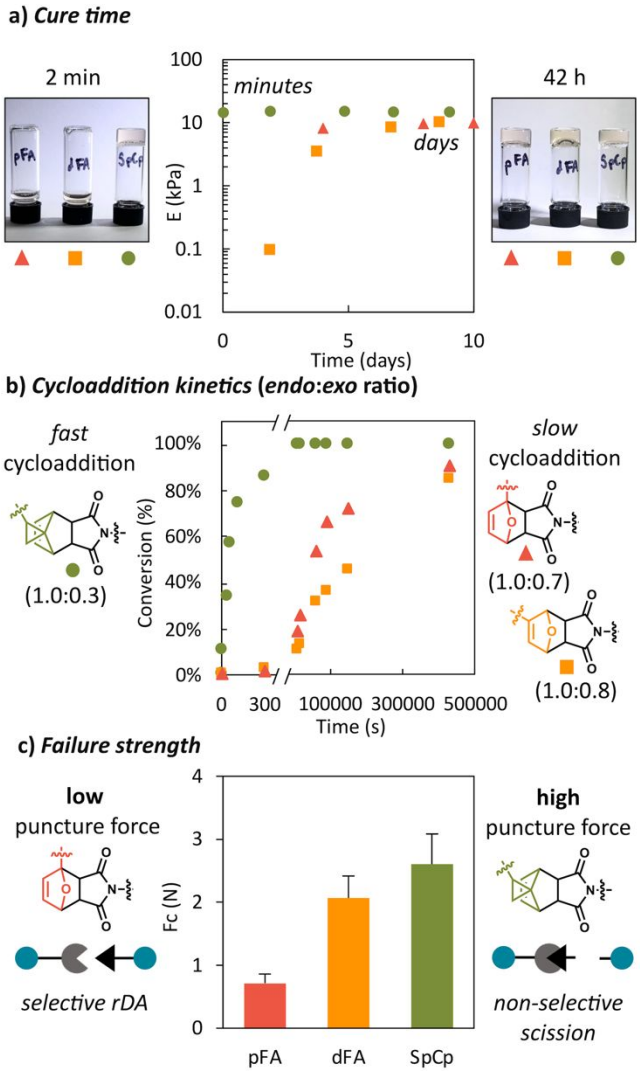

Figure 4. a) Plot of Young's modulus (E) measured via indentation as samples cured over multiple days. b) Cycloaddition kinetics of diene crosslinkers determined by ^{1}H NMR and final *endo*:*exo* ratio of adducts. Conversion and ratio of isomers determined by integration of diene signals against ethylene carbonate internal standard. c) The required puncture force (F_c) for pFA ($n = 6$), dFA ($n = 4$) and SpCp hydrogels ($n = 3$).

CONCLUSIONS

In conclusion, we have demonstrated that rational consideration of the mechanolability of DA cycloadducts plays a critical role in the resulting macroscopic properties of networks prepared from them. Specifically, we find a direct relationship between the presence of mechanolabile DA linkages and the resulting puncture force of the network. As such, by employing mechanoresistant DA adducts in place of traditional *proximal* furan–maleimide, the puncture resistance of networks was increased 3-fold. Based on the reported results of this study, we suggest that the simple substitution of traditional *proximal* furans for the *distal* regioisomer, which is commercially available, will provide a facile route to improved lifetime, utility, and mechanical durability in furan-based biomaterials while maintaining potential for thermal reversibility and dynamic behavior. Alternatively, we present a second thermally stable and mechanoresistant diene, spiro[2.4]hepta-4,6-diene, with significantly improved gelation kinetics that we anticipate will have great utility in bioprinting and cell encapsulation applications. This study highlights how mechanochemical reactivity can optimize for mechanical robustness. Conversely, we also envision that the purposeful design and use of DA mechanophores could provide unique advantages in the preparation of dynamic self-healing or stress relaxing materials that could mimic the viscoelasticity of natural tissues. Thus, the combinatorial mechanical and thermal rDA for improved dissociative stress relaxing biomimetic materials is an exciting future direction. Given the ubiquity of DA cycloadditions in the preparation of hydrogels for a variety of biomedical applications, this work demonstrates that DA cycloadduct mechanochemistry should be an important consideration in the synthetic design of devices and therapeutics.

ASSOCIATED CONTENT

Detailed descriptions of synthetic procedures, characterization of building blocks and hydrogels, puncture methods employed, and CoGEF calculations can be found in the Supplementary Information (PDF).

Videos provide examples of puncture runs with conical crack (SV1, MP4) and cone and tube-type crack (SV2, MP4) morphologies.

AUTHOR INFORMATION

Corresponding Author

*javier@chem.ucsb.edu

CONFLICTS OF INTEREST

The authors declare no competing interests.

ACKNOWLEDGMENT

The research reported here was partially supported by the BioPACIFIC Materials Innovation Platform of the National Science Foundation under award No. DMR-1933487. Use was made of computational facilities purchased with funds from the National Science Foundation (CNS-1725797) and administered by the Center for Scientific Computing (CSC). The CSC is supported by the California NanoSystems Institute and the Materials Research Science and Engineering Center (MRSEC; NSF DMR 1720256) at UC Santa Barbara. CWB and NJS were supported by the MRSEC Program of the National Science Foundation under Award No. DMR 1720256 (IRG-3). SJB would also like to thank the UCSB graduate division for financial support through a Chancellor's Fellowship.

REFERENCES

1 T. N. Gevrek and A. Sanyal, Furan-Containing Polymeric Materials: Harnessing the Diels-Alder Chemistry for Biomedical Applications. *Eur. Polym. J.* 2021, **153**, 110514. DOI: 10.1016/j.eurpolymj.2021.110514.

2 F. Cadamuro, L. Russo and F. Nicotra, Biomedical Hydrogels Fabricated Using Diels–Alder Crosslinking. *Eur. J. Org. Chem.* 2021, **2021**, 374–382. DOI: 10.1002/ejoc.202001042.

3 X. Chen, M. A. Dam, K. Ono, A. Mal, H. Shen, S. R. Nutt, K. Sheran and F. Wudl, A Thermally Re-Mendable Cross-Linked Polymeric Material. *Science* 2002, **295**, 1698–1702. DOI: 10.1126/science.1065879.

4 A. Gandini, The Furan/Maleimide Diels–Alder Reaction: A Versatile Click–Unclick Tool in Macromolecular Synthesis. *Prog. Polym. Sci.* 2013, **38**, 1–29. DOI: 10.1016/j.progpolymsci.2012.04.002.

5 E. H. Discekici, A. H. St. Amant, S. N. Nguyen, I.-H. Lee, C. J. Hawker and J. Read de Alaniz, J. *Endo* and *Exo* Diels–Alder Adducts: Temperature-Tunable Building Blocks for Selective Chemical Functionalization. *J. Am. Chem. Soc.* 2018, **140**, 5009–5013. DOI: 10.1021/jacs.8b01544.

6 M. Gregoritza and F. P. Brandl, The Diels–Alder Reaction: A Powerful Tool for the Design of Drug Delivery Systems and Biomaterials. *Eur. J. Pharm. Biopharm.* 2015, **97**, 438–453. DOI: 10.1016/j.ejpb.2015.06.007.

7 S. S. M. Konda, J. N. Brantley, B. T. Varghese, K. M. Wiggins, C. W. Bielawski and D. E. Makarov, Molecular Catch Bonds and the Anti-Hammond Effect in Polymer Mechanochemistry. *J. Am. Chem. Soc.* 2013, **135**, 12722–12729. DOI: 10.1021/ja4051108.

8 Y. Min, S. Huang, Y. Wang, Z. Zhang, B. Du, X. Zhang and Z. Fan, Sonochemical Transformation of Epoxy–Amine Thermoset into Soluble and Reusable Polymers. *Macromolecules* 2015, **48**, 316–322. DOI: 10.1021/ma501934p.

9 H.-Y. Duan, Y.-X. Wang, L.-J. Wang, Y.-Q. Min, X.-H. Zhang and B.-Y. Du, An Investigation of the Selective Chain Scission at Centered Diels–Alder Mechanophore under Ultrasonication. *Macromolecules* 2017, **50**, 1353–1361. DOI: 10.1021/acs.macromol.6b02370.

10 R. Stevenson and G. De Bo, Controlling Reactivity by Geometry in Retro-Diels–Alder Reactions under Tension. *J. Am. Chem. Soc.* 2017, **139**, 16768–16771. DOI: 10.1021/jacs.7b08895.

11 Z. Wang and S. L. Craig, Stereochemical Effects on the Mechanochemical Scission of Furan–Maleimide Diels–Alder Adducts. *Chem. Commun.* 2019, **55**, 12263–12266. DOI: 10.1039/C9CC06361G.

12 S. Wang, H. K. Beech, B. H. Bowser, T. B. Kouznetsova, B. D. Olsen, M. Rubinstein and S. L. Craig, Mechanism Dictates Mechanics: A Molecular Substituent Effect in the Macroscopic Fracture of a Covalent Polymer Network. *J. Am. Chem. Soc.* 2021, **143**, 3714–3718. DOI: 10.1021/jacs.1c00265.

13 J.-Y. Sun, X. Zhao, W. R. K. Illeperuma, O. Chaudhuri, K. H. Oh, D. J. Mooney, J. J. Vlassak and Z. Suo, Highly Stretchable and Tough Hydrogels. *Nature* 2012, **489**, 133–136. DOI: 10.1038/nature11409.

14 V. X. Truong, M. P. Ablett, S. M. Richardson, J. A. Hoyland and A. P. Dove, Simultaneous Orthogonal Dual-Click Approach to Tough, *in-Situ*-Forming Hydrogels for Cell Encapsulation. *J. Am. Chem. Soc.* 2015, **137**, 1618–1622. DOI: 10.1021/ja511681s.

15 Y. Deng, M. Huang, D. Sun, Y. Hou, Y. Li, T. Dong, X. Wang, L. Zhang and W. Yang, Dual Physically Cross-Linked κ-Carrageenan-Based Double Network Hydrogels with Superior Self-Healing Performance for Biomedical Application. *ACS Appl. Mater. Interfaces* 2018, **10**, 37544–37554. DOI: 10.1021/acsami.8b15385.

16 J. N. M. Boots, D. W. te Brake, J. M. Clough, J. Tauber, J. Ruiz-Franco, T. E. Kodger and J. van der Gucht, Quantifying Bond Rupture during Indentation Fracture of Soft Polymer Networks Using Molecular Mechanophores. *Phys. Rev. Materials* 2022, **6**, 025605. DOI: 10.1103/PhysRevMaterials.6.025605.

17 C. M. Nimmo, S. C. Owen and M. S. Shoichet, Diels−Alder Click Cross-Linked Hyaluronic Acid Hydrogels for Tissue Engineering. *Biomacromolecules* 2011, **12**, 824–830. DOI: 10.1021/bm101446k.

18 S. C. Owen, S. A. Fisher, R. Y. Tam, C. M. Nimmo and M. S. Shoichet, Hyaluronic Acid Click Hydrogels Emulate the Extracellular Matrix. *Langmuir* 2013, **29**, 7393–7400. DOI: 10.1021/la305000w.

19 L. J. Smith, S. M. Taimoory, R. Y. Tam, A. E. G. Baker, N. Binth Mohammad, J. F. Trant and M. S. Shoichet, Diels–Alder Click-Cross-Linked Hydrogels with Increased Reactivity Enable 3D Cell Encapsulation. *Biomacromolecules* 2018, **19**, 926–935. DOI: 10.1021/acs.biomac.7b01715.

20 A. H. St. Amant, D. Lemen, S. Florinas, S. Mao, C. Fazenbaker, H. Zhong, H. Wu, C. Gao, R. J. Christie and J. Read de Alaniz, Tuning the Diels–Alder Reaction for Bioconjugation to Maleimide Drug-Linkers. *Bioconjugate Chem.* 2018, **29**, 2406–2414. DOI: 10.1021/acs.bioconjchem.8b00320.

21 E. Mueller, I. Poulin, W. J. Bodnaryk and T. Hoare, Click Chemistry Hydrogels for Extrusion Bioprinting: Progress, Challenges, and Opportunities. *Biomacromolecules* 2022, Article ASAP. DOI: 10.1021/acs.biomac.1c01105 (accessed 2022-01-08).

22 C. M. Madl and S. C. Heilshorn, Rapid Diels–Alder Cross-Linking of Cell Encapsulating Hydrogels. *Chem. Mater.* 2019, **31**, 8035–8043. DOI: 10.1021/acs.chemmater.9b02485.

23 R. D. J. Froese, M. G. Organ, J. D. Goddard, T. D. P. Stack and B. M. Trost, Theoretical and Experimental Studies of the Diels-Alder Dimerizations of Substituted Cyclopentadienes. *J. Am. Chem. Soc.* 1995, **117**, 10931–10938. DOI: 10.1021/ja00149a016.

24 B. Rickborn, in *Organic Reactions*, ed. John Wiley & Sons, Inc., John Wiley & Sons, Inc., Hoboken, NJ, USA, 1998, pp. 1–393.

25 X. Hu, M. E. McFadden, R. W. Barber and M. J. Robb, Mechanochemical Regulation of a Photochemical Reaction. *J. Am. Chem. Soc.* 2018, **140**, 14073–14077. DOI: 10.1021/jacs.8b09628.

26 R. W. Barber and M. J. Robb, A Modular Approach to Mechanically Gated Photoswitching with Color-Tunable Molecular Force Probes. *Chem. Sci.* 2021, **12**, 11703–11709. DOI: 10.1039/D1SC02890A.

27 J. M. Lenhardt, A. L. Black and S. L. Craig, *gem* -Dichlorocyclopropanes as Abundant and Efficient Mechanophores in Polybutadiene Copolymers under Mechanical Stress. *J. Am. Chem. Soc.* 2009, **131**, 10818–10819. DOI: 10.1021/ja9036548.

28 I. M. Klein, C. C. Husic, D. P. Kovács, N. J. Choquette and M. J. Robb, Validation of the CoGEF Method as a Predictive Tool for Polymer Mechanochemistry. *J. Am. Chem. Soc.* 2020, **142**, 16364–16381. DOI: 10.1021/jacs.0c06868.

29 T. Sakai, T. Matsunaga, Y. Yamamoto, C. Ito, R. Yoshida, S. Suzuki, N. Sasaki, M. Shibayama and U. Chung, Design and Fabrication of a High-Strength Hydrogel with Ideally Homogeneous Network Structure from Tetrahedron-like Macromonomers. *Macromolecules* 2008, **41**, 5379–5384. DOI: 10.1021/ma800476x.

30 Y. Akagi, T. Katashima, Y. Katsumoto, K. Fujii, T. Matsunaga, U. Chung, M. Shibayama and T. Sakai, Examination of the Theories of Rubber Elasticity Using an Ideal Polymer Network. *Macromolecules* 2011, **44**, 5817–5821. DOI: 10.1021/ma201088r.

31 T. Sakai, Y. Akagi, S. Kondo and U. Chung, Experimental Verification of Fracture Mechanism for Polymer Gels with Controlled Network Structure. *Soft Matter* 2014, **10**, 6658–6665. DOI: 10.1039/C4SM00709C.

32 T. Matsunaga, T. Sakai, Y. Akagi, U. Chung and M. Shibayama, Structure Characterization of Tetra-PEG Gel by Small-Angle Neutron Scattering. *Macromolecules* 2009, **42**, 1344–1351. DOI: 10.1021/ma802280n.

33 P. Malo de Molina, S. Lad and M. E. Helgeson, Heterogeneity and Its Influence on the Properties of Difunctional Poly(Ethylene Glycol) Hydrogels: Structure and Mechanics. *Macromolecules* 2015, **48**, 5402–5411. DOI: 10.1021/acs.macromol.5b01115.

34 D. C. Rideout and R. Breslow, Hydrophobic Acceleration of Diels-Alder Reactions. *J. Am. Chem. Soc.* 1980, **102**, 7816–7817. DOI: 10.1021/ja00546a048.

35 S. Fakhouri, S. B. Hutchens and A. J. Crosby, Puncture Mechanics of Soft Solids. *Soft Matter* 2015, **11**, 4723–4730. DOI: 10.1039/c5sm00230c.

36 S. Rattan, L. Li, H. K. Lau, A. J. Crosby and K. L. Kiick, Micromechanical Characterization of Soft, Biopolymeric Hydrogels: Stiffness, Resilience, and Failure. *Soft Matter* 2018, **14**, 3478–3489. DOI: 10.1039/c8sm00501j.

37 C. W. Barney, C. Chen and A. J. Crosby, Deep Indentation and Puncture of a Rigid Cylinder Inserted into a Soft Solid. *Soft Matter* 2021, **17**, 5574–5580. DOI: 10.1039/d0sm01775b.

38 S. Rattan and A. J. Crosby, Effect of Polymer Volume Fraction on Fracture Initiation in Soft Gels at Small Length Scales, *ACS Macro Lett.*, 2019, **8**, 492–498. DOI: 10.1021/acsmacrolett.9b00086.

39 S. Fregonese and M. Bacca, Piercing soft solids: A mechanical theory for needle insertion, *J. Mech. Phys. Solids*, 2021, **154**, 104497. DOI: 10.1016/j.jmps.2021.104497.